

Non-integer and mixed integer forms in long n -alkanes observed by real-time LAM spectroscopy and SAXS

G. Ungar^{a,*}, X.B. Zeng^a, S.J. Spells^b

^aDepartment of Engineering Materials, University of Sheffield, Sheffield S1 3JD, UK

^bMaterials Research Institute, Sheffield Hallam University, City Campus, Sheffield S1 1WB, UK

Received 26 October 1999; received in revised form 8 February 2000; accepted 22 February 2000

Abstract

Application of real-time Raman longitudinal acoustic mode (LAM) spectroscopy is demonstrated in the studies of comparatively fast crystallising and transforming monodisperse polyethylene oligomers. The experiments have confirmed the structural model of the transient non-integer folded (NIF) form in long-chain n -alkane $C_{246}H_{494}$ derived previously from real-time small-angle X-ray scattering (SAXS). During crystallisation of the NIF and its subsequent isothermal transformation into the once-folded form F2 a single fundamental (LAM-1) peak of constant frequency is observed, which corresponds to the straight chain segment length exactly equal to half the full chain length. This confirms that crystalline core layers of the NIF have a constant thickness corresponding to that of the once-folded form F2. The remaining thickness making up the full lamellar periodicity thus consists of an amorphous layer made up of cilia. The constant frequency, but increasing intensity of the LAM-1 band during isothermal annealing is consistent with the cilia crystallising by re-entering the existing crystalline layers. In alkanes $C_{210}H_{422}$ and $C_{198}H_{398}$ another mechanism of transformation of the NIF into a more stable structure is observed. A new mixed-integer folded–extended (FE) phase forms instead of the pure once-folded F2 phase. Instead of re-entering the existing crystal layer, the cilia from two neighbouring NIF lamellae gather and form a third intercalated crystalline layer. The resulting superstructure contains three crystalline layers in a repeat unit. Whether one or the other of the two transformation modes take place appears to depend on factors such as fraction of folded chains in the NIF, overcrowding at the crystal–amorphous interface and chain diffusion. © 2000 Elsevier Science Ltd. All rights reserved.

Keywords: Small-angle X-ray scattering; Raman spectroscopy; Longitudinal acoustic mode

1. Introduction

It was found previously that long-chain monodisperse n -alkanes from $C_{150}H_{302}$ to $C_{390}H_{782}$ form preferentially crystalline lamellar stacks with layer spacing $l = l_E/n$, where l_E is the period of extended chain layers and $n = 1, 2, 3, \dots$ [1]. In these ‘integer’ forms, molecules adopt conformations with $n-1$ folds such that the chain ends are located at the layer surface; these conformations maximise crystallinity causing local energy minima. However real-time small-angle X-ray scattering (SAXS) experiments have shown that initially the stacks do not have integer periodicities [2]. Below the melting point of once-folded chain crystals, the transient ‘non-integer’ form (NIF) appears first, with $l_E/2 < l < l_E$. Similar observations of integer [3] and non-integer [4] forms also have been made in studies of narrow

molecular weight fractions of poly(ethylene oxide). Recent analysis of small-angle diffraction intensities suggested that the NIF lamella in fact consists of a crystalline core layer with thickness $l_E/2$ and of an amorphous layer. Initially the volume ratio between the two is as low as 2:1 (see Fig. 1).

In addition to SAXS, low-frequency-shift Raman spectroscopy has been used in the study of different folded forms of long n -alkanes [1,5]. The straight stem length l_{LAM} , as measured from the frequency of the longitudinal acoustic mode (LAM), has been found to correspond always to an integer fraction of the fully extended chain length. This observation was compatible with the information from SAXS that mature crystals, the only ones that could be studied by the LAM spectroscopy, were indeed integer folded. In the meantime improvements in photon detection efficiency have reduced drastically the spectral acquisition times, making it possible to perform time-resolved Raman LAM experiments on transient structures. Thus, we are in the position now to apply the LAM spectroscopy to study the formation and subsequent transformation of the transient

* Corresponding author. Tel.: +44-114-222-5457; fax: +44-114-222-5943.

E-mail address: g.ungar@sheffield.ac.uk (G. Ungar).

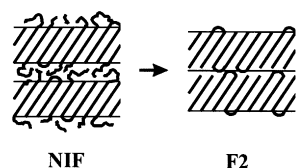


Fig. 1. Schematic representation of the non-integer form (NIF) and of the subsequent transformation to the once-folded (F2) integer form. The transformation must involve translation of half-crystallised chains in order to ensure that cilium length is that of half a chain; this enables an amorphous cilium to re-enter the crystal and make a full traverse.

NIF form in long alkanes. Amongst other things, the technique allows our model of the NIF structure to be tested independently.

2. Experimental

2.1. Materials

The long-chain *n*-alkanes used in this work were provided kindly by Drs G.M. Brooke and S. Mohammed, University of Durham, UK. For details of the synthesis see Ref. [6]. Melting temperatures were determined by DSC.

2.2. Small angle X-ray scattering (SAXS)

The in situ SAXS experiments were performed on Station 8.2 of the Daresbury Synchrotron Radiation Source. Samples for X-ray diffraction experiments were kept in thin-walled borosilicate glass capillaries. The beam was monochromatised to a wavelength of 0.16 nm and double-focused onto the detector, having a cross-section of $1 \times 0.3 \text{ mm}^2$ in the sample plane [7]. A high count rate quadrant multiwire detector was used and the sample to detector distance was 3.1 m. The capillary with the sample was held in a modified Linkam hot stage with temperature control within 0.5°C . The beam was monitored with two ionization chambers, whose reading was used for normalisation of diffracted intensities. All diffractograms were corrected for uneven channel response by dividing them with the response to homogeneous radiation of Fe^{55} . This also took care of the slice shape of the detector window, allowing the resulting curves to be treated as if recorded with a linear detector. The correction for positional non-linearity of the detector was done using a mask with equidistant concentric arc-shaped slits. The sample-to-detector distance in detector pixel units was calibrated using polycrystalline samples of a series of shorter orthorhombic *n*-alkanes.

2.3. Raman LAM spectroscopy

A Jobin–Yvon T64000 spectrometer was used in the subtractive triple-grating geometry. 514.5 nm laser exciting radiation was used and detection was by a CCD camera. A $100\times$ long working distance objective lens was used

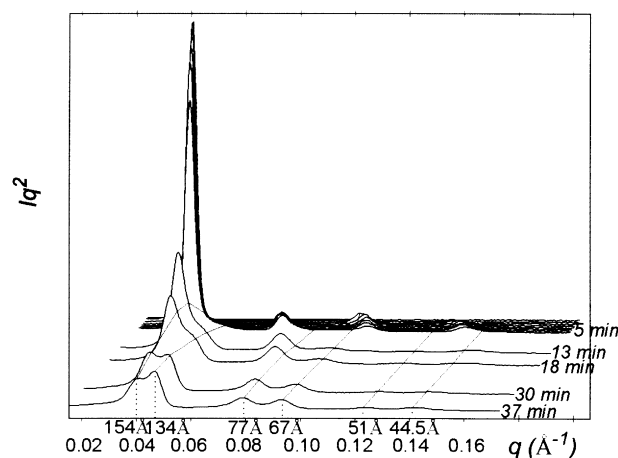


Fig. 2. Time evolution of SAXS during isothermal crystallisation of *n*- $\text{C}_{246}\text{H}_{494}$ at $T_c = 113^\circ\text{C}$ from the melt. Time t is counted from the moment of reaching T_c . Abscissas are marked in $q = 4\pi \sin\theta/\lambda$ (in \AA^{-1}) and $d = 2\pi/q$ (in \AA).

together with a $50 \mu\text{m}$ receiving slit. The samples were kept either in thin-walled glass capillaries as used in X-ray experiments or, where rapid temperature changes were required, in glass DSC pans. A specially designed Linkam T -jump stage [8] was employed for the latter type of experiments. Good signal-to-noise ratio was achieved typically with 1 min counting time. The increase in sample temperature at the focal spot was no more than 1°C , as determined from melting experiments on alkanes with known melting points.

3. Results and discussion

Fig. 2 [9] shows a series of SAXS traces recorded during isothermal crystallisation of the *n*-alkane $\text{C}_{246}\text{H}_{494}$. The strong diffraction peak and its higher orders that appear at first belong to the NIF form. The spacing is seen to decrease with time almost continuously from 190\AA initially to 134\AA , the latter value corresponding to $l_E/2$ closely, i.e. to the ‘integer’ once-folded form F2. After annealing at 113°C for 3 h, the sample is transformed completely to the F2 form with no trace of the NIF remaining (see Fig. 3). Fig. 3 shows five orders of diffraction from layers with 129\AA periodicity; this corresponds to lamellae of $\text{C}_{246}\text{H}_{494}$ chains folded exactly into two and tilted at 35° with respect to the layer normal, i.e. $l = (l_E/2) \cos 35^\circ = ((246 \cdot 1.27 + 2)/2) \cos 35^\circ = 129 \text{\AA}$. The 35° angle is the most common tilt angle in melt-crystallised long alkanes and polyethylene and is consistent with $\{201\}$ basal planes.

According to our current model of the NIF, derived from studies of electron density [9], some molecules are crystallised fully and folded exactly into two within the crystalline layer, while others traverse the crystal layer only once, leaving two long ends (cilia) in the amorphous phase. Electron density profiles reconstructed from successive small-angle

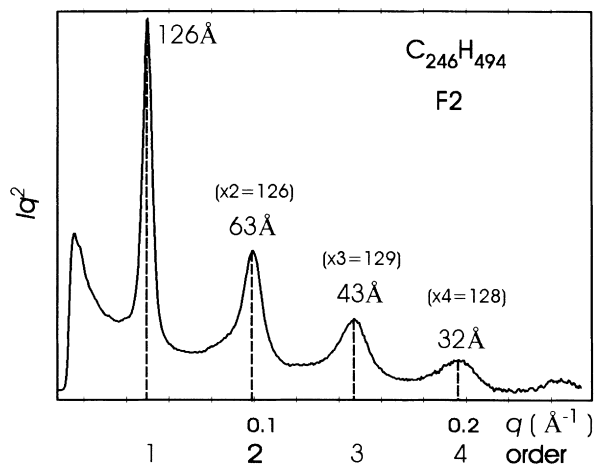


Fig. 3. SAXS trace of $n\text{-C}_{246}\text{H}_{494}$ after isothermal crystallisation/annealing for 3 hours at 113°C . The sample consists of pure once-folded F2 form. 5 diffraction orders are visible.

diffraction orders indicate further that subsequent reduction in lamellar spacing $l = l_c + l_a$ proceeds through a reduction in the amorphous thickness l_a , with the crystalline thickness l_c remaining unchanged. This implies that the NIF \rightarrow F2 transformation consists of the cilia gradually finding their way into the crystal.

3.1. Real-time Raman LAM spectroscopy of $\text{C}_{246}\text{H}_{494}$ crystallisation

In order to test the above conclusions, in this work we have carried out now real-time Raman LAM experiments capturing the process of isothermal crystallisation of $\text{C}_{246}\text{H}_{494}$. The experiment was performed at the same crystallisation temperature $T_c = 113^\circ\text{C}$ as the SAXS experiment in Fig. 2. The LAM frequency ν is an independent measure of the length of the all-*trans* sequence of the alkane chain, hence it measures the length of the chain traverse through the crystal [10–12]. Fig. 4 shows the sequence of the LAM spectra each recorded for 1 min ending at the times t indicated. There is a single sharp LAM-1 peak already after $t = 1$ min whose position ($\nu = 20 \text{ cm}^{-1}$) does not change throughout the experiment and corresponds to an all-*trans* length of $m = 124$ C-atoms; this is very close to half the chain, i.e. $246/2 = 123$ C-atoms. The relationship

$$m = 2470/\nu$$

is used, having been obtained by calibration with extended-chain long alkanes up to $\text{C}_{294}\text{C}_{590}$ [5]. This relationship is equivalent to

$$l = 3137/\nu$$

where ν is in cm^{-1} and l is in \AA . By the time the first Raman spectrum in our experiment is collected, the primary NIF crystallisation is complete already as shown by wide-angle X-ray diffraction recorded simultaneously with SAXS [9]. Further isothermal changes to the LAM spectrum amount to

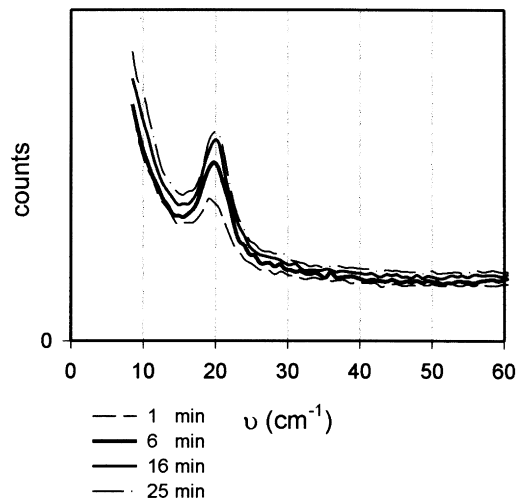


Fig. 4. Series of time-resolved Raman LAM spectra recorded during isothermal crystallisation of $n\text{-C}_{246}\text{H}_{494}$ at $T_c = 113^\circ\text{C}$ from the melt—cf. Fig. 2. Times t indicated are end-times for each timeframe, counting from the arrival at T_c . Collection time was 1 min per spectrum.

an increase only in the intensity of the LAM-1 band without any appreciable shift in its position.

The Raman spectra in Fig. 4 are consistent entirely with both the NIF structure and the NIF \rightarrow F2 transformation mechanism (Fig. 1) proposed previously on the basis of SAXS analysis. The LAM peak of the NIF form arises from the portions of the alkane chains traversing the crystalline layer. The fact that the length of these crystalline portions is only half the chain length and not larger, as the SAXS spacing of the NIF might suggest, corroborates our two-phase model.

It should be noted that the present Raman result also is consistent with our previous conclusion that the chains are tilted within the crystalline layers of the NIF. Specifically, electron density profiles of the NIF form give the value of l_c as one half of the value of l_c for *tilted* extended chain crystals [13].

Both the molecules that are folded and those that are not contribute to the LAM band, the latter presumably with half the intensity of the former. The increase in intensity of the LAM-1 band with time, seen in Fig. 4, is primarily attributed to crystallisation of the cilia. The picture derived from SAXS whereby, with post-crystallisation annealing time, l_a is reduced gradually while l_c stays constant, is compatible fully with the Raman results. It is possible, however, that a part of the increase in the LAM intensity in Fig. 4 is caused by the crystals perfecting [14]. The presence of conformational defects has been shown previously to reduce the LAM intensity [15].

The present Raman LAM results are in contrast with those by Kim and Krimm [16] on molecular weight fractions of poly(ethylene oxide). Due to its slow crystallisation, this polymer could be studied by the LAM spectroscopy without the need of short counting times. These authors have reported an initial LAM band corresponding to a

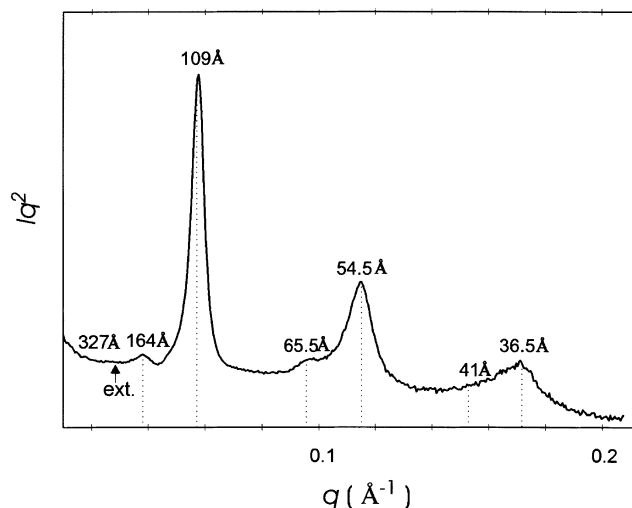


Fig. 5. SAXS trace of $C_{210}H_{422}$ after isothermal crystallisation at 111°C for 35 min, recorded at 25°C . ' $1.5l_E$ ' FE triple layers have 327 Å overall periodicity. The zero intensity first diffraction order at 327 Å is indicated. The arrow points to the position where the first-order layer reflection of the extended chain form would be expected.

straight PEO segment length intermediate between the full and one half-chain length. After prolonged annealing, this NIF band gave way to extended-chain and F2 bands. At present, the cause of the discrepancy in the LAM results in the two systems and the rate of limited polydispersity of PEO fractions are matters for speculation.

3.2. Folded–extended chain crystals of $C_{210}H_{422}$

In our recent synchrotron SAXS experiments on isothermal crystallisation of a range of *n*-alkanes, it became apparent that the shorter alkanes $C_{210}H_{422}$ and $C_{198}H_{398}$ behave somewhat differently compared with the longer ones. These shorter alkanes also pass through the NIF stage as the primary form. However, instead of transforming subsequently into the once-folded F2 phase, NIF turns into a new more complex layered phase. The SAXS trace of this new

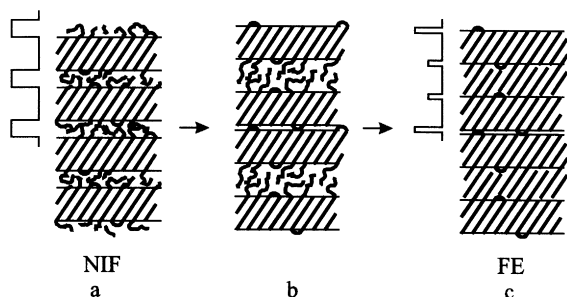


Fig. 6. Schematic representation of the transformation of the NIF form (a) to the FE form (c). (b) is not envisaged to actually occur in reality as a separate stage because of the overcrowding problem at the crystalline–amorphous interface; simultaneous chain translation and cilium crystallisation is envisaged to occur instead. Density profiles are sketched schematically on the left.

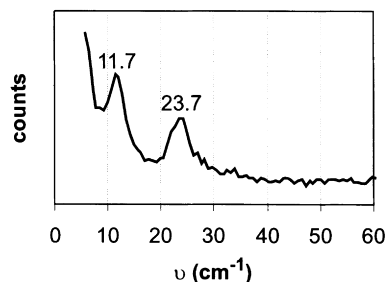


Fig. 7. Raman LAM spectrum of the mixed integer (FE) form of $C_{210}H_{422}$, with the proposed structure in Fig. 6c. The two peaks correspond to the full length and half length of an extended chain.

form in $C_{210}H_{422}$ is shown in Fig. 5. Although the strongest peaks are located at positions where one would expect the 1st, 2nd and 3rd order reflections of the 109 Å spacing of the F2 form, there are additional peaks that appear consistently at specific locations. These additional peaks are not diffraction orders of the residual NIF form: their spacings do not obey an integer ratio; their positions and intensities do not change with temperature and annealing time as do those of the NIF; and they survive even the longest annealing at the crystallisation temperature. The entire series of diffraction peaks in Fig. 5 can be indexed in fact as 2nd, 3rd, 5th, 6th, 8th and 9th orders of the fundamental layer spacing of 327 Å. This is exactly equal to $1.5l_E \cos 35^\circ$, or three times the expected spacing of the once-folded F2 form.

Preliminary electron density profiles reconstructed from measured intensities suggest the structure of the new ' $1.5l_E$ ' layer phase to be as in Fig. 6c. Two repeat units are shown, each consisting of three crystalline layers approximately $1.5l_E \cos 35^\circ$ in thickness. It is proposed that the ' $1.5l_E$ ' phase is a co-crystal of matching pairs of once-folded and extended molecules.

Raman LAM spectrum of the same sample of $C_{210}H_{422}$, taken after recording the SAXS diffractogram in Fig. 5 and without any subsequent treatment, is shown in Fig. 7. The spectrum indeed shows two clear components: one at 11.7 cm^{-1} corresponding to extended chains ($m = 211$) and another at 23.6 cm^{-1} corresponding to half the chain length ($m = 105$). This Raman result strongly supports the new mixed-integer 'folded–extended' (FE) layer structure.

It should be noted that all isothermal crystallisation in this work was carried out well below the folded-chain melting point, where no isothermal thickening to the standard extended-chain form takes place, as indeed confirmed by real-time SAXS.

In Fig. 6c the up–down orientation of folded molecules is shown as random. While it could be argued that placing the folds on the outer surfaces of a triple layer is favoured energetically, it is questionable whether such preference would be sufficient to cause effective molecular selection during the formation of the FE structure. The answer to this question is expected from planned neutron scattering experiments on a selectively deuterated alkane.

3.3. Non-integer–integer phase conversion

The suggested mechanism of conversion of the NIF into the FE form is sketched schematically in Fig. 6. As in the NIF → F2 transformation of $C_{246}H_{494}$, the amorphous cilia crystallise. However, here they do not have to find their way into the existing crystalline layers, a tortuous process, which in $C_{246}H_{494}$ takes several hours to complete and which probably involves lateral expansion and break-up of the lamellae. In the NIF → FE transformation, the cilia form a new crystalline layer of the same or similar thickness as the existing crystalline layers constituents of the NIF. The new crystalline layer is ‘shared’ between the cilia emanating from the original crystal layers on either side. This means that the half-crystallised chains from the bottom crystal layer are pulled up while those from the top layer translate downwards (see Fig. 6b). Such reorganisation makes all the cilia the correct length, $l_E/2$, for incorporation in the new crystal layer. At the same time it allows the favourable arrangement of chain ends flush with the two outermost surfaces of the triple layer unit. In the FE form, folded chains are confined to the top and bottom layers, while extended chains traverse one of the two internal interfaces as tie-chains.

The above arrangement requires that the number of folded chains be approximately one third. This condition would put strict constraints on the ability of the NIF to convert to the FE structure. If the fraction of folded chains is too low, the NIF lamellae are not able to grow due to the overcrowding of cilia at the crystalline–amorphous interface. The overcrowding problem is considered to be resolved if between one half and two third of the chains emanating from the crystal end or fold back in a tight loop at the crystal surface [17,18]. In the case of the NIF, where every non-folded chain forms a cilium at *each* end, this would mean that at least 1/3 of all chains must be tightly folded. Thus with the folded chain fraction below 1/3 the NIF cannot grow, while with it being above 1/3 the NIF → FE transformation is prevented for the lack of cilia available to fill the volume of the additional (third) crystalline layer. These tight constraints may explain why the NIF → FE transformation, which should occur more easily than the NIF → F2 conversion, is not seen in all alkanes, e.g. in $C_{246}H_{494}$. One may speculate that in $C_{246}H_{494}$ the stage of optimal folded fraction is for some reason missed irretrievably as the folded fraction continues to increase with annealing time.

While the above mechanism is somewhat speculative at this time, ongoing studies of electron density and of mixed systems appear to lend further support to our proposition.

4. Conclusions

From the results of this work one can draw two main conclusions:

(1) Application of real-time Raman LAM spectroscopy,

made possible through improved photon collection efficiency, has confirmed the structural model of the transient non-integer folded (NIF) form in long-chain *n*-alkanes derived previously from SAXS. This confirmation is based on the fact that in $C_{246}H_{494}$ during crystallisation of the NIF and its subsequent isothermal transformation into the once-folded form F2, a single LAM-1 peak of constant frequency is observed, which corresponds exactly to the straight chain segment length equal to half the full chain length. This confirms that crystalline core layers of the NIF have a constant thickness equal to that of the once-folded form F2. This is consistent with the remaining difference up to the full lamellar periodicity being taken up by an amorphous layer consisting of cilia. The constant frequency, but increasing intensity of the LAM-1 band during isothermal annealing is consistent with the cilia crystallising by re-entering the existing crystalline layers.

(2) A second mechanism of transformation of the NIF into a more stable structure is one where a mixed-integer FE phase forms instead of the pure once-folded F2 phase. Such a mixed-integer phase has not been recognised previously and it is observed now in alkanes $C_{210}H_{422}$ and $C_{198}H_{398}$. Instead of re-entering the existing crystal layer, cilia from the two neighbouring NIF lamellae gather and form a separate intercalated crystalline layer. The resulting superstructure thus contains triple layers as repeat units. Whether one or the other of the two types of transformation occurs appears to depend on factors such as folded-chain fraction in the NIF, the amount of overcrowding at the crystal–amorphous interface, and the rate of chain diffusion.

Acknowledgements

The authors wish to thank Dr G.M. Brooke of Durham University for supplying the samples of long *n*-alkanes and Dr N.A. Tuan of Jobin–Yvon, Paris, for performing the Raman experiments. This work was supported by Engineering and Physical Research Council, UK and University of Sheffield (X.B.Z.).

References

- [1] Ungar G, Stejny J, Keller A, Bidd I, Whiting MC. *Science* 1985;229:386.
- [2] Ungar G, Keller A. *Polymer* 1986;27:1835.
- [3] Kovacs AJ, Straupe C, Gonthier A. *J Polym Sci, Polym Symp* 1977; 59:31.
- [4] Cheng SZD, Chen J, Zhang A, Barley JS, Habenschuss A, Zschack PR. *Polymer* 1992;33:1140.
- [5] Ungar G. In: Lemstra PJ, Kleintjens LA, editors. *Integration of fundamental polymer science and technology*, London: Elsevier, 1988. p. 342.
- [6] Brooke GM, Burnett S, Mohammed S, Proctor D, Whiting MC. *J Chem Soc, Perkin Trans* 1996;1:1635.

- [7] Ungar G. X-ray studies using synchrotron radiation. In: Spells SJ, editor. Characterization of solid polymers, London: Chapman and Hall, 1994.
- [8] Zeng XB, Ungar G. In preparation.
- [9] Ungar G, Zeng XB, Brooke GM, Mohammed S. *Macromolecules* 1998;31:1875.
- [10] Peterlin A. *J Polym Sci, Polym Phys Ed* 1982;20:2329.
- [11] Hendra PJ, Marsden EP. *J Polym Sci, Polym Lett* 1977;15:259.
- [12] Reneker DH, Fanconi B. *J Appl Phys* 1975;46:4144.
- [13] Zeng XB, Ungar G. *Polymer* 1998;39:4523.
- [14] Gorce JP, Spells SJ. In preparation.
- [15] Strobl GR, Eckel R. *Colloid Polym Sci* 1980;258:570.
- [16] Kim I, Krimm S. *Macromolecules* 1996;29:7186.
- [17] Guttman CM, DiMarzio EA. *Macromolecules* 1982;15:525.
- [18] Balijepalli S, Rutledge GC. *Macromol Symp* 1998;133:71.